The Shape and Stretching of an Elastic Jump Rope

Melissa Strait

5.6.08

1 Introduction

This paper examines the shape and stretching of an extensible jump rope in motion. Specifically, we investigate general trends between the amount of stretch at a given point on the jump rope and the location of this point relative to the axis of rotation. We are also concerned with how the behavior of ropes with non-constant mass density differs from those with constant mass densities. In [1] the shape of an inextensible rotating jump rope is considered. Although the shape may appear similar to a parabola or hyperbolic cosine, there is actually no simple closed form description. [1] tackles this problem by modeling the jump rope using the general wave equation and then solving the resulting equations numerically. This paper follows a similar path to determine the shape and stretching of an elastic jump rope. In order to model the shape and stretching of a rapidly rotating jump rope we use the general wave equation and the resulting system of second order differential equations is solved numerically using the software Mathematica. A shooting method is used to find solutions which satisfy the boundary conditions imposed by the fixed ends of the jump rope. The solutions are graphed to illustrate the shapes of various elastic jump ropes and we then examine the stretching of the jump ropes at different points.

2 Mathematical Model

The mathematical model of the jump rope is created from the general wave equation

$$\rho(s)\mathbf{x}_{tt}(s,t) = \mathbf{T}_s(s,t) + \mathbf{a}(s,t)\rho(s) \tag{1}$$

which describes the motion and position of any one-dimensional elastic material located in three dimensions. Here

$$\mathbf{x}(s,t) = \begin{bmatrix} x(s,t) \\ y(s,t) \\ z(s,t) \end{bmatrix}$$

is a parametric description of the center of the rope. In order to illustrate the physical significance of the terms in (1), a small segment of the curve being described is shown in Figure 1. The vector $\mathbf{T}(s,t)$ represents the force experienced by the segment to the left of s due to the segment to the right of s; it is always directed tangent to the curve because of the flexible nature of a rope. We can relate $\mathbf{T}(s,t)$ to the *tension*, $T(s,t)$, in the rope by

$$\mathbf{T}(s,t) = T(s,t)\frac{\mathbf{x_s}}{||\mathbf{x_s}||}.$$

The vector $\mathbf{a}(s,t)\rho(s)$ is associated with the sum of all the body forces acting on a given section of the curve where $\rho(s)$ is the mass density of the jump rope.

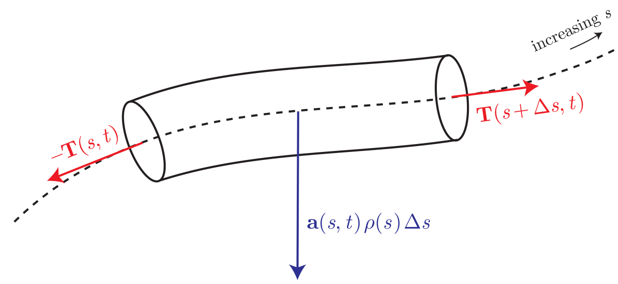

Fig. 1 *Free-body diagram of a small segment of the curve. The dashed curve is $\mathbf{x}(s,t)$, the centerline of the string, rope, or chain.*

Figure 1: A depiction of a rope described by the general wave equation taken from [1].

Before modifying this equation to model the shape of the elastic jump rope, several assumptions about the rope must be made. Using the general wave equation necessitates the assumption that the jump rope is one dimensional. For the model this is appropriate because the diameter of the jump rope is insignificant compared to its length. Additionally, we will assume that the centripetal force dominates and that effects of gravity and air-resistance can be ignored. Because we are interested in sufficiently high rotational velocities, the centripetal force will be much greater than the force of gravity. Similarly, since a jump rope has a very small surface area the effect of air-resistance is negligible compared to the dominating force. We also assume that the jump rope behaves in a linearly elastic manner and is rotated at a constant angular velocity, ω.

Because we are primarily interested in the behavior of elastic jump ropes within a certain range of rotational velocities and mass densities these assumptions are appropriate for the model. It is important to note that for insufficiently high rates of rotation, the effect of gravity cannot be ignored and the model will no longer apply. On the other hand, extremely high rotational velocities and high mass densities result in a large amount of body forces acting on the jump rope. In these cases the jump rope will undergo a great deal of strain and it might be unreasonable to assume that the material will continue to behave elastically.

Since the effect of gravity is ignored in our model, the shape of the jump rope will be static throughout its rotation. Therefore we can consider the jump rope in the rotating frame of reference to obtain a time independent model. Let the ends of the jump rope be fixed at $(0,0)$ and $(H,0)$ in the $x-y$ plane and let the x-axis be the axis of rotation. In the rotating frame of reference, the observed centrifugal force acting on a short segment of rope with length Δs is $\omega^2 y(s)\rho(s)\Delta s\hat{\mathbf{j}}$. In a linearly elastic material, the tension can be expressed as

$$T(s,t) = k(||\mathbf{x}_s|| - 1),$$

where k can be thought of as a spring constant. With these relations (1) becomes

$$\mathbf{0} = \frac{\partial}{\partial s}\left(\frac{k(||\mathbf{x}_s|| - 1)\mathbf{x}_s}{||\mathbf{x}_s||}\right) + \omega^2 y(s)\rho(s)\hat{\mathbf{j}},$$

providing a description of the rotating elastic jump rope. For a jump rope with length L, the system of equations to be solved is

$$\begin{aligned} 0 &= \frac{\partial}{\partial s}\left(\frac{k(||\mathbf{x}_s|| - 1)x_s}{||\mathbf{x}_s||}\right), \\ 0 &= \frac{\partial}{\partial s}\left(\frac{k(||\mathbf{x}_s|| - 1)y_s}{||\mathbf{x}_s||}\right) + \omega^2 y(s)\rho(s), \end{aligned}$$

subject to boundary conditions $x(0) = 0, x(L) = H, y(0) = 0$, and $y(L) = 0$.

3 Solution Technique

Since there is no closed form solution to the system of differential equations that model the jump rope, the problem must be approached numerically. We want to use a shooting method to determine the solution to this boundary value problem, but must first determine approximate initial conditions where we can begin the method. In order to obtain these values, we treat the problem as an initial value problem. Using the software, Mathematica, we write the method *GraphSolution* which takes in user specified values for the initial conditions and then returns a plot of the solution for these parameters. The built in *Manipulate* function allows us to visually determine the effects of modifying the initial conditions and obtain solutions to the differential equations that approximate solutions satisfying the boundary conditions.

Not all initial values are appropriate to consider for this problem. The functions $y_s(s)$ and $x_s(s)$ are related to the amount of stretching of the jump rope at point s by the equation

$$\text{Stretch}(s) = ||\mathbf{x}_s|| - 1 = \sqrt{y_s^2(s) + x_s^2(s)} - 1. \tag{2}$$

Therefore only initial values of y_s and x_s that result in Stretch(0) > 0 provide a valid physical description of this problem. In order to more easily incorporate this constraint into the solution method, the initial condition $y'(0)$ is not directly modified in the method *GraphSolution*, but varied through the parameter Stretch(0) related to $y'(0)$ and $x'(0)$ by (2). This graphical approximation technique easily allows for the discovery of different modes of a jump rope.

The graphically determined initial conditions are then used as the starting values for a shooting method to solve the boundary value problem. This is completed using Mathematica's *NDSolve* function and specifying the shooting method option. This technique is capable of finding solutions for both jump ropes with constant mass density and those with mass densities given by a continuous function.

Although Mathematica's shooting method takes a significant amount of time to compute the non-constant case, the nature of the problem that concerns us does not necessitate a large number of trials and therefore algorithm efficiency is not a priority. When $L = 5$ and $H = 1$, the solutions calculated using this method were found to deviate from the boundary conditions by approximately 10^{-6} or less. This accuracy declines, however, as the complexity of the problem is increased by considering non-constant mass densities or higher modes of the jump rope.

4 Results

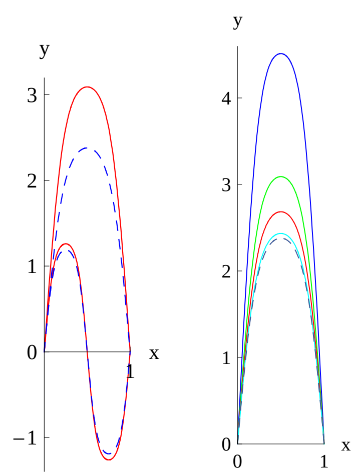

Figure 2: On the left we compare the shape of an elastic jump rope with $k = 10$ (solid) and an inextensible jump rope (dotted). Both jump ropes have $\rho(s) = 1, \omega = 1$, and $L = 5$. Two modes for both cases are shown. On the right we see how the shape of the jump rope varies with k while the other parameters remain the same as mentioned above. The solid plots in blue, green, red, and cyan correspond to $k = 5, k = 10, k = 20$, and $k = 100$ respectively. The inextensible jump rope (dotted) is again shown for comparison.

4.1 Jump ropes with Constant Mass Density

Using the technique above, we calculate the curve of the jump rope for different parameters. There are several intuitive relationships between the parameters and the jump rope shape that our solutions support. First we can compare the shape of the linearly elastic jump rope with the inextensible jump rope in the left plot in Figure 2. The results of the model coincide with our visual expectation of an elastic jump rope.

Additionally we can examine how increasing angular velocity or mass density affects the shape. Although not pictured here, the model predicts that the amplitude of the jump rope will increase as these parameters are increased, as expected. Finally, we can examine how the "spring constant" and the shape are related. This data is shown in the right plot in Figure 2. As the spring constant increases and the rope becomes stiffer, the behavior of the rope approaches the behavior of the inextensible case.

Now we use the model to examine the extent of stretching at each point on the jump rope. Recall that once we obtain the equations, $x(s)$ and $y(s)$, which describe the shape of the jump rope, the stretching of the jump rope at point s is given by Equation (2). Two modes of a jump rope with constant mass density and colored according to the amount of stretching at a given point are shown in Figure 3. Examining these two plots illustrates several aspects of how stretching occurs on the jump rope. First, notice that in both configurations the maximum amount of stretch occurs at points closest to the axis of rotation. Conversely, the points of least amount of stretching occur at peaks of the jump rope shape. For the constant density case we can also observe that all points on a given jump rope shape which are the same vertical distance away from the axis of rotation will undergo the same amount of stretching. This, however, is not the case for jump ropes of non-constant mass density. Comparing the two graphs in Figure

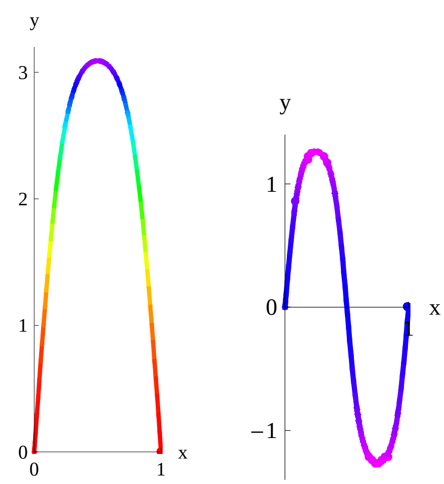

Figure 3: On the left the first mode of an elastic jump rope with $k = 10, \omega = 1, \rho(s) = 1$, and $L = 5$ is shown. The red areas indicate the highest amount of stretch (approximately 0.42) while the purple areas indicate the smallest amount of stretch (approximately 0.03). The right plot shows the second mode of the same jump rope colored using the same scale.

3 also allows us to see that the amount of maximum stretch for the two jump rope modes is different. The first mode, where the jump rope only meets the axis rotation at the endpoints, has a larger maximum stretch value than the second mode of the jump rope. We see a continuation of this trend if modes 3 and 4 are examined. Table 1 shows

the maximum and minimum stretch values for all four modes and indicates that less stretching occurs for jump rope configurations that cross the axis of rotation a greater number of times. Intuitively this makes sense because in these configurations the rope is generally closer to the center of rotation and therefore the apparent centrifugal forces are smaller.

Table 1: Stretch Values for Different Jump Rope Modes

Mode Number	Minimum Stretch	Maximum Stretch
1	0.0297	0.4197
2	0.0070	0.0831
3	0.0031	0.0356
4	0.0017	0.0197

4.2 Jump ropes with Non-constant Mass Density

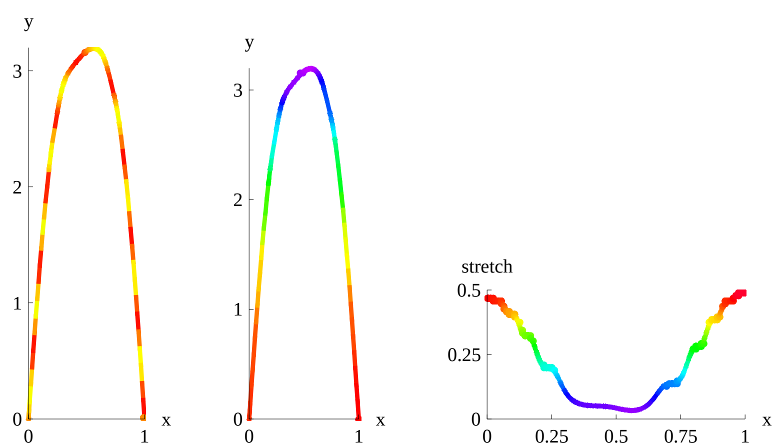

Figure 4: These plots correspond to a jump rope with $\rho(s) = 1.1 + \sin(4\pi s), \omega = 1, k = 10$, and $L = 5$. On the left the shape of the jump rope is colored according to the mass density at a given point (red corresponds to $\rho(s) = 0.1$, yellow to $\rho(s) = 2.1$. The middle plot shows the same jump rope colored according to the amount of stretch at a given point (red corresponds to stretch(s) approximately 0.5 and purple corresponds to stretch(s) approximately 0.03. On the right, the x axis is plotted vs. the amount of stretch in the jump rope.

Now non constant mass density cases are considered. Figure 4 depicts a jump rope with a mass density given by

$$\rho(s) = 1.1 + \sin(4\pi s).$$

As seen previously for the constant mass density jump rope, the points of greatest stretching occur at places closest to the axis of rotation and the points of least stretching occur at points farthest from the axis. This example highlights that for jump ropes with non-constant mass density, two points on the jump rope that are the same distance away from the axis of rotation will not necessarily be stretched the same amount, as was the case for the constant mass density jump rope. We calculate that for $s_1 = 0$ and $s_2 = L$, $y(s_1) = y(s_2) = 0$; however, $\text{stretch}(s_1) = 0.470$ and $\text{stretch}(s_2) = 0.487$. This behavior is even more apparent in the following example. A jump rope with

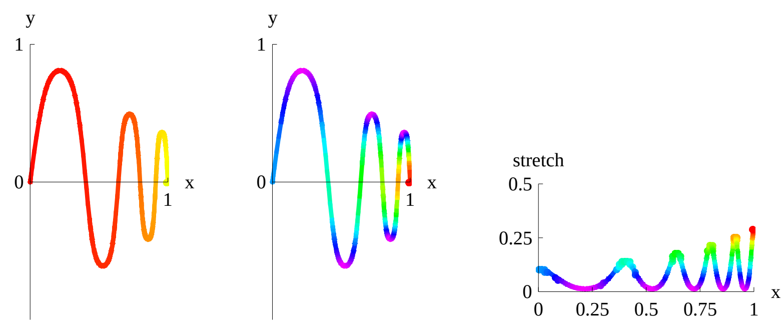

Figure 5: These plots correspond to a jump rope with $\rho(s) = 2e^{\frac{2}{3}s}, \omega = 1, k = 10$, and $L = 5$. On the left the shape of the jump rope is colored according to the mass density at a given point (red corresponds to $\rho(s) = 2$, yellow to $\rho(s) = 56$. The middle plot shows the same jump rope colored according to the amount of stretch at a given point (red corresponds to $\text{stretch}(s)$ approximately 0.3 and purple corresponds to $\text{stretch}(s)$ approximately 0.01. On the right, the x axis is plotted vs. the amount of stretch in the jump rope.

$$\rho(s) = 2e^{\frac{2}{3}s}$$

is shown in Figure 5. It is clear that the right endpoint on the axis of rotation is undergoing a much greater amount of stretch than the left endpoint. Incorporating non-constant mass densities creates a much more complicated stretching pattern. Even so, the maximum amount of stretching always occurs at some point on the axis of rotation.

5 Conclusion

Our model of a rotating elastic jump rope succeeding in providing an intuitively correct image for varying values of k and ω. It also provided a means of determining the amount of stretching at a given point on the jump rope. By considering the stretching of a jump rope with constant mass density we were able to determine that the most stretching occurs at points on the axis of rotation and the least stretching occurs at points farthest away. Also, jump rope configurations that cross the axis of rotation at more points experience less stretching. The non-constant mass density case created a less predictable stretching pattern, although the maximum amount of stretching still occurred at points on the axis of rotation.

References

[1] Yong, Darryl, *Strings, Chains, and Ropes*. SIAM Review, Vol. 48, No. 4, pp771-781.